

Recoil Studies of Nuclear Reactions Induced by Heavy Ions*

JOHN M. ALEXANDER AND LESTER WINSBERG

Lawrence Radiation Laboratory, University of California, Berkeley, California

(Received September 15, 1960)

The mechanism of nuclear reactions induced by heavy ions was investigated by measuring the recoil ranges of Tb^{149} , At^{211} and other alpha-emitting isotopes of At and neighboring elements and by determining the cross sections for the formation of Tb^{149} and At^{211} .

Recoil ranges were consistent with compound-nucleus formation at all energies studied for the following reactions: $\text{Pr}^{141}(\text{C}^{12}, 4n)\text{Tb}^{149}$, $\text{Ce}(\text{N}^{14}, xn)\text{Tb}^{149}$, $\text{La}^{139}(\text{O}^{16}, 6n)\text{Tb}^{149}$, $\text{La}^{139}(\text{O}^{18}, 8n)\text{Tb}^{149}$, and $\text{Ba}(\text{Ne}^{22}, pxn)\text{Tb}^{149}$. A similar result was obtained for the reaction $\text{Pr}^{141}(\text{O}^{16}, 2p6n)\text{Tb}^{149}$ at 138 and at 146 Mev and for the reactions $\text{Au}^{197}(\text{O}^{16}, 2pxn)$ and $3pxn\text{At}$, Po at energies below 100 Mev. The excitation functions of the $(\text{HI}, xn)\text{Tb}^{149}$ reactions seem to be characteristic of an evaporation process but have smaller peak cross sections than do the excitation functions of the reactions $\text{Ba}(\text{Ne}^{22}, pxn)\text{Tb}^{149}$ or $\text{Pr}^{141}(\text{O}^{16}, 2p6n)\text{Tb}^{149}$. We conclude that most reactions probably involve charged-particle emission. The reaction

$\text{Ba}(\text{Ne}^{22}, pxn)\text{Tb}^{149}$ seems to occur with much greater probability than the reaction $\text{Ba}(\text{Ne}^{20}, pxn)\text{Tb}^{149}$.

In many cases the compound-nucleus mechanism cannot account for our results. Partial momentum transfer is observed in the reactions $\text{Au}^{197}(\text{O}^{16}, 2pxn)$ and $3pxn\text{At}$, Po at energies above 100 Mev. Partial momentum transfer also occurs when Bi is bombarded at energies 1.3 times the barrier energy or greater. Reactions of Bi with heavy ions (Ne^{20} is possible exception) at energies near the Coulomb barrier produce At^{211} with greater recoil energy than expected from a compound-nucleus mechanism. Apparently, particles are emitted in the backward direction. Near the barrier the cross section for the production of At^{211} by C^{12} , O^{16} , and Ne^{20} bombardment comprises about $\frac{1}{4}$ the value calculated for compound-nucleus formation. Therefore, the cross section for all noncompound-nucleus reactions must comprise a large fraction of the total interaction cross section. The experiments with Pb as a target are also consistent with this conclusion.

INTRODUCTION

THE recoil properties of the products of a nuclear reaction provide direct evidence for the reaction mechanism. In the preceding paper we studied a number of reactions induced by heavy ions (HI) for the purpose of determining the energy dependence of the range and range straggling of heavy nuclei.¹ In this paper we use these results to study the mechanism of heavy-ion-induced spallation reactions by the recoil technique.

The interpretation of many nuclear-reaction studies has been based on the assumption of compound-nucleus formation. In this model the incident projectile is absorbed by the target nucleus to form an excited compound state.² The subsequent decay of the compound nucleus has been described by evaporation theory.²⁻⁴ For example, excitation functions and energy spectra of emitted particles have been analyzed with these models to determine the density of states in excited nuclei.^{3,4} Many of these interpretations would be significantly changed by the presence of nuclear reactions that take place by noncompound-nucleus processes. However, few experiments have severely tested the limits of applicability of the compound-nucleus model.

The measurement of the recoil properties of the products provides a test of compound-nucleus formation. The products of low-energy nuclear reactions fall into three distinct groups: (a) the small particles, e.g.,

nucleons, alpha particles, etc., (b) the fission products, and (c) the spallation products.

The energies of recoil and the angular distributions of the small particles and fission products are strongly affected by the de-excitation process as well as the initial impact of the projectile and target. The interpretation of these measurements involves assumptions concerning the nature of the decay of excited nuclei. However, the average recoil energy of a spallation product is determined mainly by the initial impact and is only slightly affected by the decay of the excited nucleus. The *distribution* of recoil energies and the angular distribution of the spallation products are determined both by the initial interactions and by subsequent de-excitation processes. Therefore, measurements of these distributions can furnish information about the initial interaction and about the process of de-excitation. Donovan, Harvey, and Wade have made such studies of several reactions induced by deuterons and alpha particles.⁵

In this and the preceding paper¹ we present measurements of the range distribution of some spallation products from heavy-ion-induced reactions. These reactions and the types of experiments that were performed are listed in Table I. The bombarding energies and the approximate values of the recoil energies are also given in the table.

ANALYSIS OF RESULTS

Two types of experiments were performed. In the differential method we used thin targets and thin Al catcher foils. In the integral method, targets of thickness comparable to the range were employed. Targets of compounds of Cs, Ba, La, and the elements Ce, Re,

* This work was performed under the auspices of the U. S. Atomic Energy Commission.

¹ L. Winsberg and J. M. Alexander, preceding paper [Phys. Rev. **121**, 518 (1961)].

² J. Blatt and V. F. Weisskopf, *Theoretical Nuclear Physics* (John Wiley & Sons, Inc., New York, 1952).

³ I. Dostrovsky, Z. Fraenkel, and G. Friedlander, Phys. Rev. **116**, 683 (1959). Further references are given here.

⁴ I. Dostrovsky, Z. Fraenkel, and L. Winsberg, Phys. Rev. **118**, 781 (1960). Further references are given here.

⁵ P. F. Donovan, B. G. Harvey, and W. H. Wade, Phys. Rev. **119**, 218, 225 (1960).

TABLE I. Summary of nuclear reactions studied.

Nuclear reaction ^a	Product	Type of experiment	Beam energies (Mev)	Approximate recoil energies (Mev)	Reference
Pr ¹⁴¹ (C ¹² , 4n)	Tb ¹⁴⁹	differential	55 to 82	4 to 8	1, this work
Ce(N ¹⁴ , xn)	Tb ¹⁴⁹	differential	66 to 112	6 to 10	1, this work
La ¹³⁹ (O ¹⁶ , 6n)	Tb ¹⁴⁹	differential	87 to 104	9 to 10	1
La ¹³⁹ (O ¹⁸ , 8n)	Tb ¹⁴⁹	differential	122	13	1
Ba(Ne ²⁰ , pxn)	Tb ¹⁴⁹	differential	161 to 197	<13 to 26	this work
Ba(Ne ²² , pxn)	Tb ¹⁴⁹	differential	166 to 223	21 to 29	1
Pr ¹⁴¹ (O ¹⁶ , 2p6n)	Tb ¹⁴⁹	differential	115 to 146	7 to 14	this work
Au ¹⁹⁷ {(C ¹² , xn) (C ¹² , pxn)}	At Po	diff. and int.	65 to 120	4 to 7	1
Pt{(N ¹⁴ , xn) (N ¹⁴ , pxn)}	At Po	diff.-int.	90 to 143	6 to 9	1
Ir{(O ¹⁸ , xn) (O ¹⁸ , pxn)}	At Po	differential	72 to 183	6 to 15	1
Re{(Ne ²² , xn) (Ne ²² , pxn)}	At Po	differential	125	13	1
Au ¹⁹⁷ {(O ¹⁶ , xn) to (O ¹⁶ , 3pxn)}	Fr to Po	diff. and int.	80 to 159	6 to 9	1, this work
Bi ²⁰⁹ (C ¹² to Ne ²² , ?)	alpha emitters	diff. and int.	59(C ¹²) to 182(Ne ²⁰)	3 to 11	this work
Pb(C ¹² and O ¹⁶ , ?)	alpha emitters	integral	76(C ¹²) to 135(O ¹⁶)	4 to 6	this work

^a The notation indicates the maximum number of protons that can be emitted.

Ir, Au, Pb, and Bi were exposed to beams (C¹², N¹⁴, O¹⁶, O¹⁸, Ne²⁰, and Ne²²) from the Berkeley heavy-ion linear accelerator. The reaction products, Tb¹⁴⁹, At, Po, and several other alpha emitters were observed. These products were chosen because they are easily detected by direct measurement of the alpha radioactivity in the various foils. The experimental details are given in the preceding paper.¹

The experiments employing the integral method give the average range, R_0 . The analysis of the integral and differential experiments for Gaussian range distributions has already been described.¹

Many of the differential experiments indicated range distributions that are quite different from a Gaussian.

Therefore we have analyzed these experiments in terms of three quantities: R_0 , the average range, R_M , the median range, and ρ_M , a measure of the range distribution. The average range was calculated from

$$R_0 = \sum_i (t + \frac{1}{2}t_i) f_i,$$

where t_i is the thickness of a given catcher foil, t is the total thickness of other catcher foils before this foil, and f_i is the fraction of the total activity found in the given foil. The median range, R_M , was obtained from a graph on a probability scale of F_t (the fraction of the activity that passed through absorbers of total thickness t) as a function of t . Here R_M is the t value for which we have $F_t = \frac{1}{2}$ as obtained from a smooth curve drawn

TABLE II. Recoil properties of Tb¹⁴⁹ in Al.

Possible nuclear reaction	Beam energy, E_b (Mev)	Total degrader (mg/cm ² Al)	Target thickness (μ g/cm ² Al)	Average range, R_0 (mg/cm ² Al)	Median range, R_M (mg/cm ² Al)	Straggling parameter ρ_M	E_{eq} (Mev)	E_{eq}/E_{CN}	ρ_M/ρ_{CN}
Pr ¹⁴¹ (C ¹² , 4n)	76.4	34.5	47	0.490	0.480	0.32	5.9	1.01	1.1
Pr ¹⁴¹ (C ¹² , 4n) ^a	81.7	31.4	72	0.60 ^b	0.53 ^b	0.60 ^b	7.7 ^b	1.23 ^b	2.1 ^b
				0.50	0.46	0.36	6.1	1.0	1.3
Ba(Ne ²⁰ , pxn) ^{c, d}	161.4	13.4	65	1.2		0.2	19	1.0	1.0 to 1.4
Ba(Ne ²⁰ , pxn) ^{c, d}	180.0	8.3	64	1.4		0.2	22	1.0	1.0 to 1.4
Ba(Ne ²⁰ , pxn) ^{c, d}	197.2	3.3	70	1.50		0.20	26.0	1.10	1.3
Pr ¹⁴¹ (O ¹⁶ , 2p6n)	115.2	21.6	12	0.540	0.55		6.7	0.60	
Pr ¹⁴¹ (O ¹⁶ , 2p6n)	137.6	12.8	47	0.946	0.950	0.20	13.4	1.01	1.0
Pr ¹⁴¹ (O ¹⁶ , 2p6n)	145.6	9.4	49	0.987	0.986	0.21	14.2	1.01	1.0

^a Some activity from nuclides of half-period other than 4.1 hr was also observed.

^b Some spurious alpha activity appeared to be present, possibly due to activation of the foils. The first entry is for the uncorrected data; the second entry was obtained with the "extra" activity subtracted.

^c Components of half-period about 19 hr and less than about 3 hr were also present.

^d These values correspond to the long-range group only (see Fig. 1), for which a symmetrical range distribution was assumed.

through the experimental data. The tangent to the probability plot at $t=R_M$ was used to specify ρ_M (see "Analysis" section in preceding paper¹).

We have classified our experimental results (see Table I) into two groups. The experiments in group 1 (given in the preceding paper¹) satisfied the following requirements: (a) Gaussian distribution of ranges and (b) nuclear reactions of the type (HI, xn) and (HI, pxn) . We assume that these criteria select those reactions that occur by compound-nucleus formation. In calculating the recoil energies for these cases the velocity of the final product was taken to be that of the center of mass. This, of course, is expected for a compound-nucleus mechanism if the average recoil velocity is not changed by the decay of the compound nucleus. From these experiments we determined the range and range straggling of the product nuclei as a function of energy.¹ The internal consistency of the results justified the assumption of compound-nucleus formation. The experiments in group 2 do not satisfy one or both of the above requirements. In this paper we utilize all these results for an understanding of the nuclear-reaction mechanisms. The results of the group-2 differential experiments for Ba and Pr targets are presented in Table II, for Au targets in Table III, and for Bi targets in Table IV. Results of integral experiments for Bi targets are given in Table V and for Pb targets in Table VI.

From the range-energy curves (Fig. 4, reference 1) each value of R_0 is associated with an energy designated E_{eq} . The range measurements in Bi and Pb were converted to Au by means of Eqs. (23) and (24) in the preceding paper.¹ The quantity E_{CN} is the average recoil energy if a compound nucleus is formed [Eq. (8), reference 1], i.e., $E_{CN} = E_b A_b A_R / (A_b + A_T)^2$.

The approximate value of the straggling parameter if a compound nucleus is formed is denoted as ρ_{CN} . The value of ρ_{CN} was obtained from Fig. 6 of reference 1 for the measured value of R_0 . In the case of reactions

TABLE III. Recoil properties of At and Po in Al from O^{16} Bombardment of Au.^a

Beam energy (Mev)	E_{eq} (Mev)	E_{eq}/E_{CN}	ρ_M/ρ_{CN}
80.4	5.8	1.00	1.0
90.8	5.9	0.91	1.1
100.5	7.0	0.98	1.0
104.8	7.0	0.93	1.1
120.8	7.8	0.92	1.3
140.6	8.8	0.89	1.4
158.6	9.2	0.84	1.4
158.8	9.0	0.82	1.5

^a See Table V and Fig. 5 of preceding paper (reference 1).

leading to the formation of Tb^{149} a correction was made for the effect of the specific nuclear reaction by means of Eqs. (16), (19), and (20) of reference 1. In the case of the other reactions, ρ_{CN} was directly read off a curve drawn through the uncorrected experimental values of ρ in Fig. 6 of reference 1. If a nuclear reaction occurs by compound-nucleus formation, E_{eq}/E_{CN} and ρ_M/ρ_{CN} must be unity.

The physical significance of the ratio E_{eq}/E_{CN} can be illustrated by a simple example. Let us consider the reaction (O^{16}, He^4). If the alpha particle is emitted along the beam direction with the velocity of the incident ion, then $\frac{3}{4}$ of the incident momentum is transferred to the struck nucleus, and $E_{eq}/E_{CN} \cong 9/16$. Similarly, if the alpha particle is emitted in the direction opposite to the beam but with the same velocity, then $E_{eq}/E_{CN} \cong 25/16$. In either case, we would conclude that a compound-nucleus reaction did not occur. On the other hand, if the alpha particle is emitted with the velocity of the center of mass, E_{eq}/E_{CN} will equal unity.

The measured range straggling will also be influenced by the reaction mechanism. If the recoiling atoms have a unique recoil velocity along the beam direction, the straggling parameter will have the value caused by the stopping process and by foil inhomogeneities. The

TABLE IV. Recoil properties of At and Po in Al from heavy-ion reactions with Bi.

Projectile	Beam energy, E_b (Mev)	Total degrader (mg/cm ² Al)	Target thickness (μ g/cm ² Bi)	Average range, R_M (mg/cm ² Al)	Median range, R_M (mg/cm ² Al)	Straggling parameter ρ_M	E_{eq} (Mev)	E_{eq}/E_{CN}	ρ_M/ρ_{CN}
C ¹²	58.8	44.0	22	0.237	0.221	0.43	3.4	1.11	1.5
C ¹²	65.0	40.9	22	0.300	0.277	0.43	4.3	1.28	1.5
C ¹²	69.2	38.7	22	0.274	0.263	0.42	4.0	1.11	1.5
C ¹²	104.2	16.2	20	0.219	0.198	0.75	3.1	0.57	2.7
N ¹⁴	75.9	35.2	85	0.409	0.381	0.45	6.0	1.33	1.7
N ¹⁴	83.0	32.4	110	0.342	0.333	0.41	5.0	1.01	1.5
O ¹⁶	84.6	31.7	22	0.679	0.689	0.38	10.9	1.93	1.7
O ¹⁸	83.3	39.2	22	0.392	0.318	0.55	5.8	0.94	2.1
O ¹⁸	92.3	36.6	22	0.470	0.454	0.57	7.0	1.03	2.3
Ne ²⁰	98.2	27.8	22	0.304 ^a	0.291	0.43	4.4	0.56	1.5
				0.320	0.304	0.43	4.6	0.58	1.5
Ne ²⁰	119.4	23.5	85	0.298 ^a	0.275	0.57	4.3	0.45	2.0
				0.280	0.261	0.56	4.0	0.42	2.0
Ne ²²	120.8	28.0	20	0.658	0.634	0.40	10.4	0.99	1.7

^a The recoil properties changed with time. The first row gives the result of the observations made less than 12 hours after the end of bombardment. The second row gives the observations made 2 to 4 days later.

TABLE V. Integral-range data from heavy-ion reactions with Bi.

Projectile	Beam energy, E_b (Mev)	Total degrader (mg/cm ² Al)	Target thickness (mg/cm ² Bi)	Min av range, R_0 (mg/cm ² Bi)	Max av range, R_0 (mg/cm ² Bi)	Min E_{eq} (Mev)	Max E_{eq} (Mev)	Min E_{eq}/E_{CN}	Max E_{eq}/E_{CN}
C ¹²	63.2	41.9	1.143	0.54	0.54	4.2	4.2	1.28	1.28
C ¹²	64.8	41.0	1.248	0.50	0.59	3.9	4.5	1.16	1.34
C ¹²	67.3	39.7	0.990	0.53	0.55	4.1	4.3	1.17	1.23
C ¹²	71.2	37.6	1.049	0.50	0.51	4.0	4.0	1.08	1.08
C ¹²	80.4	32.2	2.945	0.42	0.47	3.3	3.7	0.79	0.89
C ¹²	81.4	31.6	0.971	0.39	0.52	3.1	4.1	0.73	0.97
C ¹²	94.0	23.5	1.143	0.32	0.53	2.6	4.1	0.53	0.84
C ¹²	94.7	22.9	3.404	0.31	0.42	2.6	3.4	0.53	0.69
C ¹²	101.4	18.2	3.136	0.30	0.39	2.4	3.1	0.46	0.59
C ¹²	105.5	15.3	1.049	0.35	0.49	2.8	3.8	0.51	0.70
C ¹²	107.4	13.8	1.058	0.36	0.48	2.9	3.7	0.52	0.67
C ¹²	116.5	6.6	3.136	0.35	0.49	2.8	3.8	0.47	0.64
C ¹²	117.7	5.6	0.908	0.33	0.40	2.7	3.2	0.45	0.53
N ¹⁴	84.6	31.7	1.482	0.65	0.69	4.9	5.2	0.97	1.03
N ¹⁴	111.9	19.1	2.26	0.42	0.52	3.4	4.1	0.51	0.62
N ¹⁴	135.2	6.2	2.461	0.32	0.45	2.6	3.6	0.33	0.45
O ¹⁶	110.0	23.5	2.26	0.52	0.56	4.0	4.3	0.54	0.59
O ¹⁶	145.7	9.4	2.461	0.33	0.41	2.7	3.3	0.28	0.34
Ne ²⁰	159.4	13.9	0.88	0.49	0.50	3.8	3.9	0.30	0.30
Ne ²⁰	181.8	7.8	0.88	0.42	0.48	3.3	3.8	0.23	0.26

evaporation process causes additional range straggling. This effect has been estimated for nucleon evaporation in reference 1. These combined effects are included in ρ_{CN} . If the distribution of recoil velocities is greater than that for nucleon evaporation from a compound nucleus, ρ_M will be larger than ρ_{CN} . This effect can arise in two ways: (a) evaporation of particles heavier than nucleons, or (b) a distribution of velocities from the initial impact, i.e., from noncompound-nucleus reactions.

In addition to the recoil measurements, a limited number of cross-section measurements are reported below for the production of Tb¹⁴⁹ and At²¹¹. These nuclides were identified by observations of the half-life.

DISCUSSION

We have studied some reactions that lead to the production of Tb¹⁴⁹ and several that lead to At and Po products. For the Tb¹⁴⁹ studies it is possible to specify the number of nucleons emitted in the reaction and the maximum number of protons that could have been emitted. In the latter case it is not known whether protons were emitted singly or in aggregates such as deuterons, alpha particles, etc. In the reactions of Ba with

Ne²⁰ and Ne²² and of Pr with O¹⁶, Tb¹⁴⁹ is a cumulative product, i.e., may also have been formed indirectly from beta decay of Dy¹⁴⁹ in addition to direct formation. In these reactions nuclear fission is probably not a serious competitor. The studies of At and Po are quite different in that identification of the observed nuclides was not usually possible with our techniques. Also the competition from the fission processes is certainly an important aspect of these studies. We will discuss the Tb¹⁴⁹ studies first, then the At and Po experiments.

(HI,xn)Tb¹⁴⁹ Reactions

Most recoil studies of the (HI,xn)Tb¹⁴⁹ reactions resulted in Gaussian range distributions and, therefore, are in the group-1 classification. Three types of evidence point to a compound-nucleus mechanism for these reactions: (a) The measured ranges from several different reactions give rise to one curve when plotted against E_{CN} . (b) The values of the range of each reaction extrapolated to the threshold also lie on this curve. (c) The measured values of ρ for these reactions are a function of the range and are in qualitative agreement with stopping theory.¹ For other reactions the values of ρ vary widely (see below).

TABLE VI. Integral-range data from heavy-ion reactions with Pb.

Projectile	Beam energy (Mev)	Total degrader (mg/cm ² Al)	Target thickness (mg/cm ² Pb)	Min av range, R_0 (mg/cm ² Pb)	Max av range, R_0 (mg/cm ² Pb)	Min E_{eq}	Max E_{eq}	Min E_{eq}/E_{CN}	Max E_{eq}/E_{CN}
C ¹²	75.8	34.9	0.968	0.49	0.50	3.9	3.9	0.98	0.98
C ¹²	91.1	25.4	0.967	0.55	0.55	4.3	4.3	0.90	0.90
C ¹²	109.2	12.4	0.974	0.53	0.54	4.1	4.2	0.71	0.73
O ¹⁶	97.1	27.9	1.077	0.72	0.74	5.4	5.6	0.82	0.85
O ¹⁶	134.9	13.9	1.077	0.52	0.60	4.1	4.6	0.45	0.50

Several studies of the reaction $\text{Pr}^{141}(\text{C}^{12}, 4n)\text{Tb}^{149}$ did not result in Gaussian range distributions. In one experiment two successive foils far beyond the most active foil contained the same amount of activity (approximately 10% of the peak value). We assumed that this activity was due to activation of these catcher foils and, therefore, that all the foils were similarly activated. The corrected data from this experiment are listed as the first entry in Table II. A similar correction was made for the second entry. The "raw" data and the data with the "extra" activity subtracted are given. Within this uncertainty the results of both experiments are consistent with compound-nucleus formation.

The N^{14} irradiation of CeO_2 targets was reported to result in products with short ranges and a non-Gaussian range distribution.⁶ We have repeated these studies with Ce metal targets as well as the CeO_2 previously used. The energy of the alpha particles from the CeO_2 experiments was found to be greater than 6 Mev, compared to 3.95 Mev for Tb^{149} .⁷ The energy and decay period of the alpha activity produced from Ce-metal targets were characteristic of Tb^{149} . The range distributions observed from Ce-metal targets were all Gaussian. These results are given in reference 1. The CeO_2 targets must have contained heavy-element impurities: hence, the results reported with these targets⁶ are incorrect.

Ba(Ne^{20} and Ne^{22} , $p\alpha n$) Reactions⁸

The cumulative production of Tb^{149} recoil atoms has been observed in reactions of Ne^{20} and Ne^{22} with Ba. Of the several Ba isotopes in the target, Ba^{138} with a 71.7% abundance is probably the most important for the bombarding energies in this study. The Ne^{22} experimental results were consistent with a Gaussian range distribution and were included in the group-1 experiments reported in the preceding paper.¹ The results of the Ne^{20} bombardments, which are quite different from those for Ne^{22} , are given in Table II and are shown in Fig. 1.

Two very distinct range groups can be seen in Fig. 1 for the Ne^{20} experiments. Values of R_0 and ρ_M were calculated for the longer range group by assuming it to have a symmetrical range distribution. The values of $E_{\text{eq}}/E_{\text{CN}}$ and ρ_M/ρ_{CN} for the long-range group are approximately unity. The products in the short-range group were stopped in the first catcher foil, which was 0.9 mg/cm² Al thick. Therefore, these ranges are less than this amount. From Fig. 1 we see that the products are about equally divided between the two groups. These results are further complicated by the presence

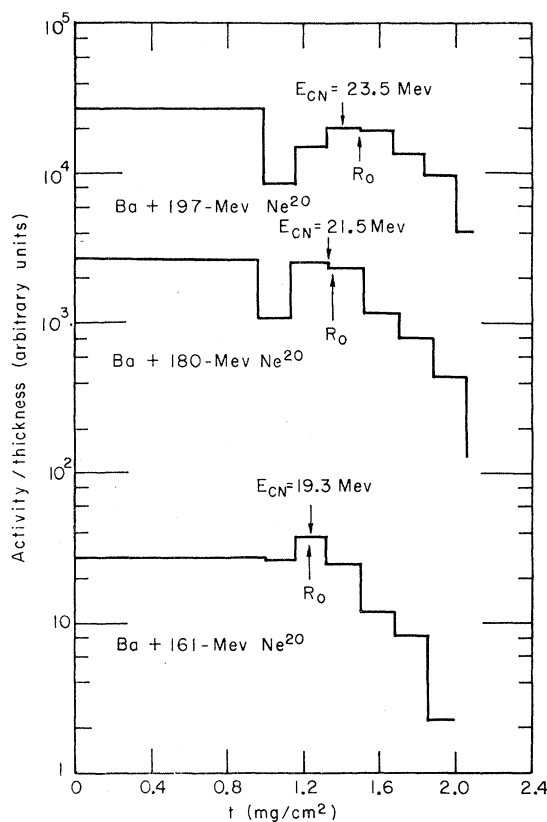


FIG. 1. Differential range studies of the reaction $\text{Ba}(\text{Ne}^{20}, p\alpha n)\text{Tb}^{149}$. Total absorber thickness is denoted by t . The average range of the long-range group is designated by the arrows labeled R_0 . Average ranges expected for compound-nucleus formation are shown by the arrows labeled E_{CN} .

of half-lives smaller and larger than 4.1 hr in both groups. We did not collect sufficient data to identify the shorter lived components. The longer lived component decayed with a half-life of approximately 20 hr. The nuclide Tb^{151} does decay with this half-life, but its branching ratio⁷ for alpha-particle emission ($3 \times 10^{-40}\%$) is too small to account for our results. No measurement was made of the alpha-particle energies. Therefore, heavy element impurities may account for the short-range products, as in the study of the $\text{Ce}(\text{N}^{14}, \alpha n)\text{Tb}^{149}$ reaction.

The cross section for the formation of Tb^{149} from Ba is about ten times greater for Ne^{22} than for Ne^{20} in the energy region that we have explored (see later discussion). We are unable to explain this striking difference.

$\text{Pr}^{141}(\text{O}^{16}, 2p6n)\text{Tb}^{149}$

The production of Tb^{149} from Pr^{141} by O^{16} bombardment has a special interest because of the possibility of alpha-particle emission. The results of several studies of this reaction are given in Table II and shown in Fig. 2. At the higher bombarding energies, the range distribution is Gaussian and both $E_{\text{eq}}/E_{\text{CN}}$ and ρ_M/ρ_{CN}

⁶ J. M. Alexander and L. Winsberg, *Proceedings of the Second Conference on Reactions between Complex Nuclei, Gallinburg, Tennessee* [John Wiley & Sons, New York (to be published)].

⁷ D. Strominger, J. M. Hollander, and G. T. Seaborg, *Revs. Modern Phys.* **30**, No. 2 (1958).

⁸ For consistency of notation we denote each reaction by the maximum number of protons that can be emitted.

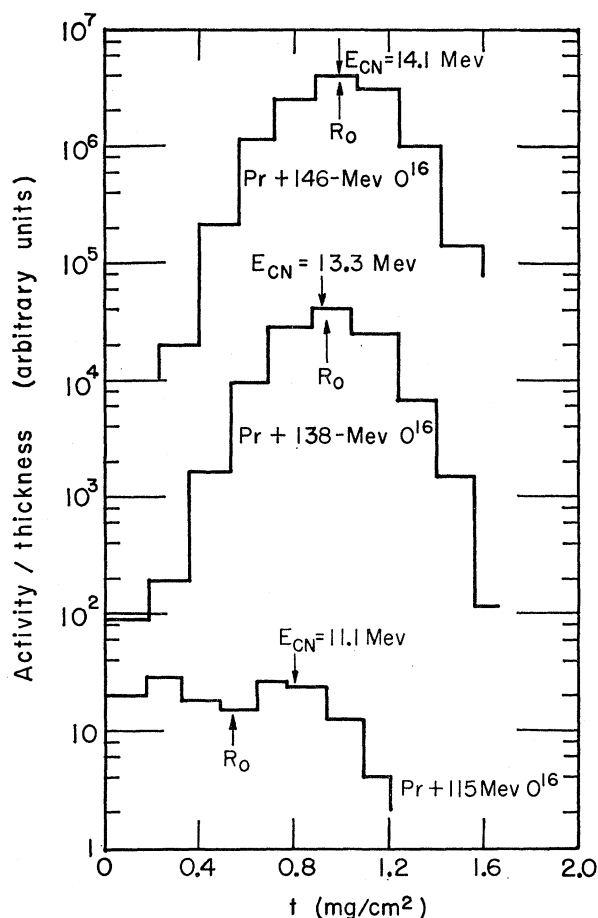


FIG. 2. Differential range studies of the reaction $\text{Pr}^{141}(\text{O}^{16}, 2p6n)\text{-Tb}^{149}$. Total absorber thickness is denoted by t . Average ranges are designated by the arrows labeled R_0 . Average ranges expected for compound-nucleus formation are shown by the arrows labeled E_{CN} .

are essentially unity. These results are evidence for compound-nucleus formation.

For 115-Mev O^{16} ions, the range distribution is very broad and not Gaussian, and the value of E_{eq}/E_{CN} is much less than unity. From the range distribution shown in Fig. 2, it appears that only about one-half the observed activity can be explained by compound-nucleus formation. The products with ranges less than the value of R_0 may be due to heavy-element impurities (see above).

Cross Sections for Tb^{149} Production

As a by-product of the range measurements, we also obtained values of the cross section for the formation of Tb^{149} . The branching ratio for alpha decay is approximately 10%.⁹ Complete excitation functions have not been obtained for any reaction. The beam intensity was monitored by a Faraday cup, which may have systematic errors as large as 40%. All of the Tb^{149} experiments

⁹ L. Winsberg, Bull. Am. Phys. Soc. 3, 406 (1958).

were of the differential-range type, and the targets were of necessity very thin. For these several reasons, the absolute values of the cross section may be in error by as much as 50%. Nevertheless, these fragmentary results do shed some light on the nature of the reactions.

The values of the cross section are shown in Fig. 3 as a function of the quantity $(E_b A_T / (A_b + A_T) + Q) / n$. The bombarding energy is denoted by E_b , and the mass number by A , the mass difference between reactants and products by Q , and the number of nucleons emitted by n . The subscript b is for the bombarding particle, and T is for the target. The values of Q for Fig. 3 are calculated for reactions in which the nucleons are emitted singly. The points shown by open symbols represent reactions in which charged particles can be emitted; closed symbols are for reactions in which only neutrons are emitted. The quantity $E_b A_T / (A_b + A_T) + Q$ is the energy left in the center-of-mass system after completion of the reaction. If all of this energy is given to the emitted nucleons, the abscissa of Fig. 3 gives the average kinetic energy of these nucleons. Where the target element has several isotopes, the plotted points are

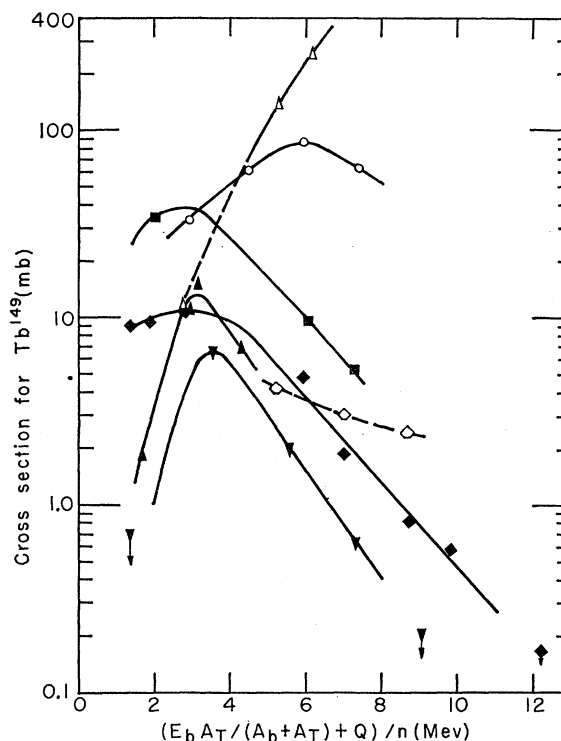


FIG. 3. The cross section for Tb^{149} production as a function of the maximum kinetic energy available in the center-of-mass system, $E_b A_T / (A_b + A_T) + Q$, divided by the number of nucleons emitted, n . Closed symbols are for (H,Xn) reactions: square, $\text{Pr}^{141}(\text{C}^{12}, 4n)\text{Tb}^{149}$; diamond, $\text{Ce}^{140}(\text{N}^{14}, 5n)\text{Tb}^{149}$; triangle, $\text{La}^{139}(\text{O}^{16}, 6n)\text{Tb}^{149}$; inverted triangle, $\text{La}^{139}(\text{O}^{18}, 8n)\text{Tb}^{149}$. Open symbols are for reactions in which charged particles can be emitted: pentagon, $\text{Ba}^{138}(\text{Ne}^{20}, 8n)\text{Tb}^{149}$; circle, $\text{Ba}^{138}(\text{Ne}^{22}, 10n)\text{Tb}^{149}$; triangle, $\text{Pr}^{141}(\text{O}^{16}, 2p6n)\text{Tb}^{149}$. Values for reactions that occur by compound-nucleus formation, according to the recoil measurements, are connected by solid lines. The other cases are connected by dashed lines.

based on the most abundant isotope (mass 138 in the case of Ba and mass 140 in the case of Ce).

Several features in Fig. 3 are noteworthy:

(a) The $(\text{HI}, xn)\text{Tb}^{149}$ reactions have much lower peak cross sections than the reactions $\text{Pr}^{141}(\text{O}^{16}, 2p6n)\text{Tb}^{149}$ or $\text{Ba}^{138}(\text{Ne}^{22}, p10n)\text{Tb}^{149}$. In the latter two reactions, charged particles can be emitted.

(b) The average available kinetic energy of the emitted nucleons at the peak value of the cross section is about 3 Mev for (HI, xn) reactions and is equal to or greater than 6 Mev for the reactions $\text{Pr}^{141}(\text{O}^{16}, 2p6n)\text{Tb}^{149}$ and $\text{Ba}^{138}(\text{Ne}^{22}, p10n)\text{Tb}^{149}$.

(c) The values of the cross section for the production of Tb^{149} from Ne^{20} bombardment of Ba are much smaller than those from Ne^{22} bombardment of the same target.

The recoil properties indicate that many of the reactions studied occur by compound-nucleus formation. The cross-section values in Fig. 3 for those reactions that appear to occur by this mechanism are connected by solid lines. If we assume that the cross section for compound-nucleus formation is given by crude barrier-penetration calculations,² it is possible to draw some conclusions about the nature of the decay of the compound nucleus.

The maximum cross sections for $(\text{HI}, xn)\text{Tb}^{149}$ reactions are all less than about 1/20 of the calculated cross section for compound-nucleus formation.¹⁰ We conclude that reactions predominate in which one or more charged particles are emitted. Further evidence for this conclusion is the magnitude of the peak cross sections for the reactions $\text{Ba}(\text{Ne}^{22}, pxn)\text{Tb}^{149}$ and $\text{Pr}^{141}(\text{O}^{16}, 2p6n)\text{Tb}^{149}$ (cumulative production of Tb^{149}). These reactions appear to be much more probable than those involving only neutron emission. Measurements of the cross section for neutron production also indicate that the emission of charged particles is important.¹¹

$\text{Au}^{197}(\text{O}^{16}, 2pxn \text{ or } 3pxn)\text{At, Po}$

We have studied the formation of alpha-emitting isotopes of At and neighboring elements by O^{16} irradiation of Au. Decay curves indicate the presence of many components, and no attempt was made to identify individual products. We assume that most of these products are isotopes of At and Po. The results are given in Table V and Fig. 5 of the preceding paper and in Table III here. For incident O^{16} energies of about 100 Mev or less, the values of $E_{\text{eq}}/E_{\text{CN}}$ and ρ_M/ρ_{CN} are approximately unity. As the incident energy is increased, the value of $E_{\text{eq}}/E_{\text{CN}}$ decreases and of ρ_M/ρ_{CN} increases significantly. These results are evidence for the occurrence of noncompound-nucleus processes which take place with increasing importance as the bombarding energy is increased.

¹⁰ T. D. Thomas, Phys. Rev. **116**, 703 (1959).

¹¹ E. L. Hubbard, R. M. Main, and R. V. Pyle, Phys. Rev. **118**, 507 (1960).

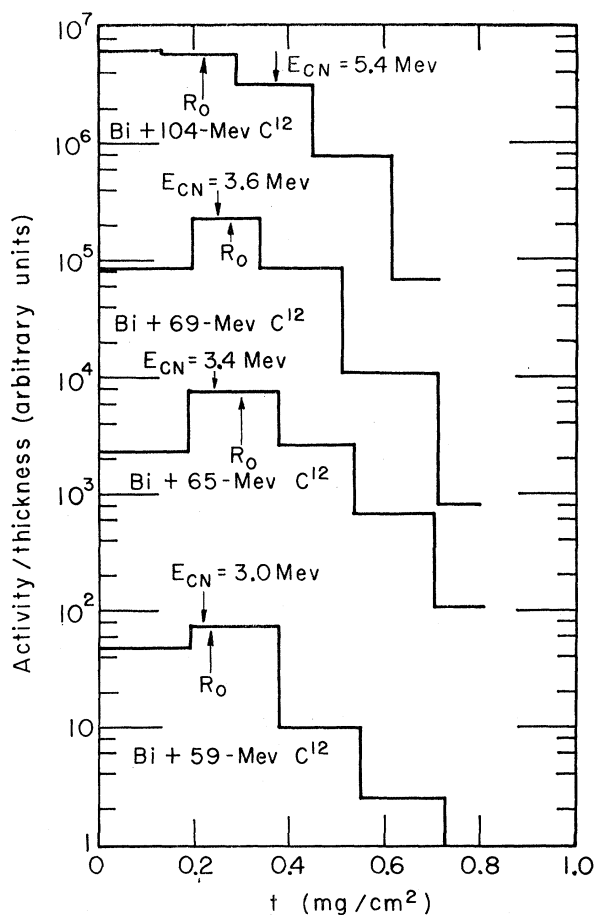


FIG. 4. Differential range studies of the reaction $\text{Bi}^{209}(\text{C}^{12}, ?)\text{At, Po}$. Total absorber thickness is denoted by t . Average ranges are designated by the arrows labeled R_0 . Average ranges expected for compound-nucleus formation are shown by the arrows labeled E_{CN} .

Bombardments of Bi and Pb

In the experiments given here we have observed the gross alpha-particle activity produced in heavy-ion bombardments of Bi and Pb. From consideration of the decay periods and alpha-particle branching ratios one would expect most of the observed nuclides to be spallation products of Po, At, Em, and possibly Fr. These species could be formed directly or from radioactive decay of short-lived parents. Indeed, we did observe very complex decay curves in many experiments. Fission is more probable from a compound nucleus with its high excitation energy than from the less excited products of interactions involving incomplete momentum transfer. Thus, these experiments are expected to be sensitive to noncompound-nucleus processes.

The results of differential experiments with Bi targets are given in Table IV. Table V summarized the integral experiments. Integral experiments with Pb targets are presented in Table VI. The measured range values often varied considerably with time. The extreme values are given in Tables V and VI.

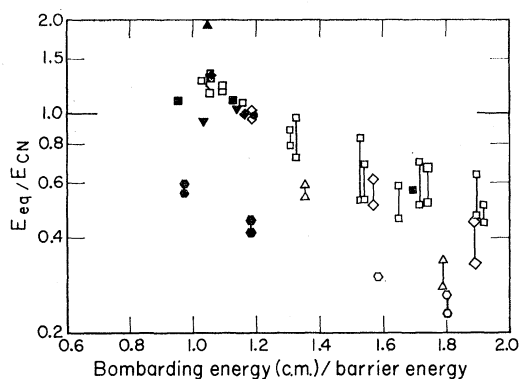


FIG. 5. Values of E_{eq}/E_{CN} for the reaction $\text{Bi}(\text{HI}, ?)\text{At}$, Po vs the incident energy divided by the barrier energy. Here E_{eq} is the recoil energy corresponding to a measured range and E_{CN} is the recoil energy if a compound nucleus is formed. Closed symbols are from differential experiments and open symbols are from integral experiments. The symbols for various projectiles are: square, C^{12} , diamond, N^{14} , triangle, O^{16} , inverted triangle, O^{18} , hexagon, Ne^{20} , and circle, Ne^{22} .

In all of these experiments, the gross alpha radioactivity decayed with half-lives greater than about 10 min. The decay curves indicated the presence of many nuclides when the incident-beam energy was greater than approximately 1.3 times that of the Coulomb barrier (r_0 taken to be 1.5 fermis). For bombarding energies less than this amount, the decay curves could usually be resolved to show the presence of a prominent 7.3-hr half-period. We assigned this activity to 7.3-hr At^{211} , which has an alpha-branching ratio of 41%.⁷ Donovan has verified this assignment by measuring the energy of these alpha particles for a 65-Mev C^{12} irradiation of Bi^{209} .¹²

We have studied the reactions of C^{12} with Bi^{209} at a number of bombarding energies. Histograms of the differential experiments are shown in Fig. 4. From this figure we see that all of the range distributions are very broad and unsymmetrical. For this reason the integral method was used only to measure R_0 . In Fig. 4 we note that at the highest incident energy the measured average range is less than the range expected if a compound nucleus is formed. For incident C^{12} energies of 59 to 69 Mev, the observed value of the average range is larger than that expected from compound-nucleus formation (see Table IV and Fig. 4). We have confirmed this result by integral range measurements (see Table V).

Very similar recoil behavior was observed for Bi^{209} reactions with N^{14} , O^{16} , O^{18} , and Ne^{22} . The results are summarized in Fig. 5. For all projectiles studied, the value of E_{eq}/E_{CN} is less than unity for incident energies more than about 1.3 times the barrier energy. For all projectiles, with the possible exception of Ne^{20} , the value of E_{eq}/E_{CN} is greater than or about equal to unity for incident energies near that of the barrier. In Fig. 6, range histograms for the reactions of O^{16} and N^{14} with

Bi are compared to those experiments with similar values of E_{CN} that were used to establish the range-energy relationship. Clearly, the average range and the width of the distribution are much greater for the Bi reactions.

Further information concerning these nuclear reactions with Bi is provided by the excitation functions. The cross sections for the formation of At^{211} as a function of the bombarding energy divided by the barrier energy are given in Fig. 7. If no clear resolution of the decay curve was possible, an upper limit to the 7.3-hr activity was obtained, as indicated by the points with an arrow

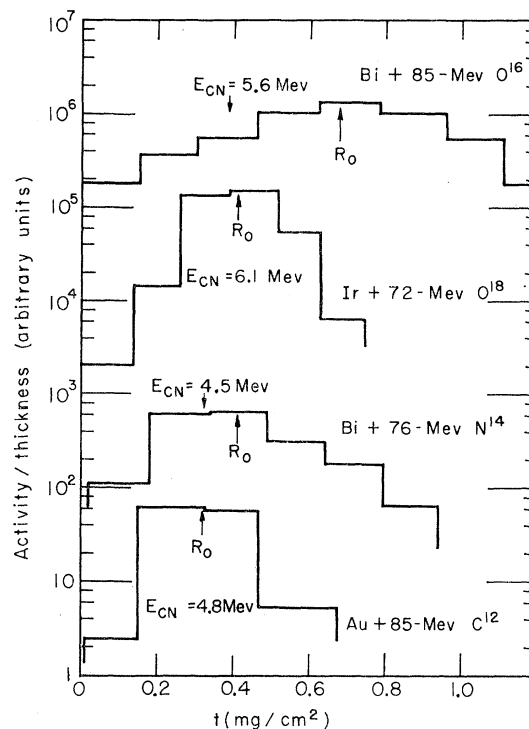


FIG. 6. Differential range studies of At and Po produced in various reactions. Average ranges are designated by the arrows labeled R_0 . For the Bi experiments, the arrows labeled E_{CN} show the average range expected for compound-nucleus formation. The experiments with Ir and Au targets were used to determine the energy dependence of range and range straggling. Hence, the arrows for R_0 and E_{CN} coincide for these cases.

pointing downward. Although the measurements are fragmentary, except for C^{12} , several statements can be made: (a) At energies near the Coulomb barrier the cross section for At^{211} production by C^{12} , O^{16} , and Ne^{20} is about one-fourth that calculated for compound-nucleus formation,¹⁰ (b) For incident energies equal to or slightly greater than the barrier, C^{12} , O^{16} , and Ne^{20} form At^{211} in much higher yield than N^{14} , O^{18} , and Ne^{22} .

The recoil measurements indicate that compound-nucleus formation is certainly not the major mechanism of these reactions ($\rho_M/\rho_{CN} > 1$ even though $E_{eq}/E_{CN} \sim 1$ in some cases). This is not surprising because the fission

¹² P. F. Donovan, Bell Laboratories, Murray Hill, New Jersey (private communication).

reaction is expected to result in high probability from compound nuclei that are formed. The products that we have observed are those that survive fission competition. Therefore they are more likely to result from noncompound-nucleus processes. Several nucleons must be transferred from the projectile to the target to form the nuclides that we have observed. The high cross section for the formation of At^{211} —only one of the possible products from multiple-nucleon transfer processes—indicates that noncompound-nucleus reactions comprise a large fraction of all the reactions.

The projectiles, C^{12} , O^{16} , and Ne^{20} , which may have structures consisting of bound alpha particles, are particularly effective in forming At^{211} . This suggests the possibility of alpha-particle transfer to the target nucleus.

The fact that $E_{\text{eq}}/E_{\text{CN}}$ is less than unity for the higher initial energies indicates that particles must be emitted preferentially in the forward hemisphere. In order to explain values of $E_{\text{eq}}/E_{\text{CN}}$ that are greater than unity, particles must be emitted in the backward hemisphere in the center-of-mass system. For this type of reaction, the recoil nucleus can obtain more momentum than the incident beam particle. This can result either from an angular distribution that is symmetric about 90° in the center-of-mass system [reference 1, Eqs. (10) and (11)] or from a preferred emission of particles in the backward direction. Using the exact form of Eq. (10), we have calculated the maximum possible value of $E_{\text{eq}}/E_{\text{CN}}$ for the reaction of 84.6-MeV O^{16} with Bi^{209} to be 1.38 (This value is obtained if the products are At^{211} and C^{14} .) This is approximately 30% less than the experimental value of 1.93 (see Table IV). If the particles are emitted backwards, the maximum possible value of $E_{\text{eq}}/E_{\text{CN}}$ is 3.45. We conclude that the particles are emitted preferentially in this direction. It is interesting that these reactions occur only for incident energies nearly equal to the energy of the Coulomb barrier. The projectiles with these low kinetic energies must have small impact parameters if they are to react. Therefore, the promptly emitted particles should be directed preferentially backwards.

A few studies were made of heavy-ion reactions with

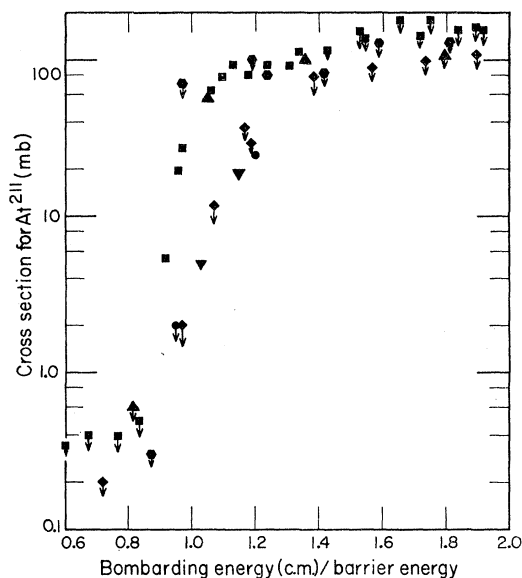


Fig. 7. Cross section for the reactions $\text{Bi}^{209}(\text{HI},?)\text{At}^{211}$ vs the incident energy divided by the barrier energy. Symbols for various heavy ions are: square, C^{12} , diamond, N^{14} , triangle, O^{16} , inverted triangle, O^{18} , hexagon, Ne^{20} , and circle, Ne^{22} . Symbols with arrows attached designate upper limits.

Pb (see Table V). The results are similar to those for Bi in that $E_{\text{eq}}/E_{\text{CN}}$ is less than unity for high incident energies. Also $E_{\text{eq}}/E_{\text{CN}}$ increases as the incident energy decreases. A further study of these reactions should prove very interesting.

ACKNOWLEDGMENTS

We wish to thank Dan O'Connell, assisted by Arthur Johns and Gordon Steers, for very careful and painstaking work in preparing our target foils. We are grateful to the operating crew of the heavy-ion accelerator and especially to Jack Gavin for the bombardments. For maintenance of the counting equipment we are indebted to Ken Russell, and for help with the counting we thank Mrs. M. F. Gazdik. We are grateful to Lawrence Altman, Peter Axel, John Huiizenga, Earl Hyde, and Wladyslaw Swiatecki for helpful discussions and critical reading of the manuscripts.